ACS chemical biology

Articles

pubs.acs.org/acschemicalbiology

Mutagenesis of Isopentenyl Phosphate Kinase To Enhance Geranyl Phosphate Kinase Activity

Mark F. Mabanglo,[†,§] Jian-Jung Pan,[†] Binita Shakya,[‡] and C. Dale Poulter*[,†]

[†]Department of Chemistry, University of Utah, 315 South 1400 East, Salt Lake City, Utah 84112, United States

[‡]Department of Biochemistry, University of Utah School of Medicine, 15 North Medical Drive, Salt Lake City, Utah 84112, United States

Supporting Information

ABSTRACT: Isopentenyl phosphate kinase (IPK) catalyzes the ATP-dependent phosphorylation of isopentenyl phosphate (IP) to form isopentenyl diphosphate (IPP) during biosynthesis of isoprenoid metabolites in Archaea. The structure of IPK from the archeaon *Thermoplasma acidophilum* (THA) was recently reported and guided the reconstruction of the IP binding site to accommodate the longer chain isoprenoid monophosphates geranyl phosphate (GP) and farnesyl phosphate (FP). We created four mutants of THA IPK with different combinations of alanine substitutions for Tyr70, Val73, Val130, and Ile140, amino acids with bulky side chains that limited the size of the side chain of the isoprenoid phosphate substrate that could be accommodated in the active site. The mutants had substantially increased GP kinase activity, with 20−200-fold increases in k_{cat}^{GP} and 30−130-fold increases in k_{cat}^{GP}/K_M^{GP} relative to those of wild-type THA IPK. The mutations also resulted in a 10^6-fold decrease in k_{cat}^{IP}/K_M^{IP} compared to that of wild-type IPK. No significant change in the kinetic parameters for the cosubstrate ATP was observed, signifying that binding between the nucleotide binding site and the IP binding site was not cooperative. The shift in substrate selectivity from IP to GP, and to a lesser extent, FP, in the mutants could act as a starting point for the creation of more efficient GP or FP kinases whose products could be exploited for the chemoenzymatic synthesis of radiolabeled isoprenoid diphosphates.

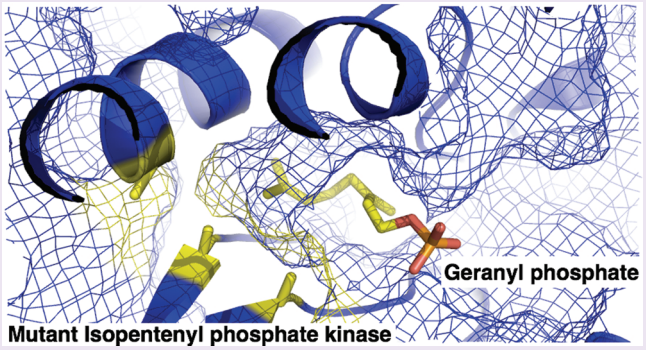

Isopentenyl phosphate kinase (IPK) is a recently identified enzyme in the modified mevalonate (MVA) pathway in Archaea that catalyzes the ATP-dependent phosphorylation of isopentenyl phosphate (IP) to produce isopentenyl diphosphate (IPP), one of two building blocks for the biosynthesis of isoprenoid compounds.[1] IPK and a putative phosphomevalonate decarboxylase are thought to complement the absence of phosphomevalonate kinase and diphosphomevalonate decarboxylase in the archaeal MVA pathway. This is accomplished by the conversion of phosphomevalonate to IPP via two consecutive steps that are the reverse of those found in the classical MVA pathway (Figure 1). As in the classic eukaryotic MVA pathway and the deoxyxylulose phosphate (DXP) pathway found in bacteria and plant chloroplasts, the IPP produced by the archaeal MVA pathway undergoes condensation reactions catalyzed by prenyltransferases to produce the vast number of isoprenoid compounds necessary to sustain life.[2−5]

The crystal structures of IPK from three archaeal organisms have been determined.[6,7] In particular, the structure of IPK from *Methanocaldococcus jannaschii* (MJ) guided the creation of mutants with observed kinase activities for the 15-carbon isoprenoid farnesyl phosphate (FP).[7] These variants contained different combinations of mutations located in the IP binding site that gave rise to their ability to bind and phosphorylate FP to form farnesyl diphosphate (FPP). While production of FPP by these mutants was confirmed using a coupled IPK-sesquiterpene synthase assay and GC−MS,[8] the mutants were not characterized kinetically, and kinase activities for the 10-carbon isoprenoid geranyl phosphate (GP) were not reported.

In this paper, we describe mutants of IPK from *Thermoplasma acidophilum* (THA) with significant GP kinase (GPK) activity, as well as weaker FP kinase (FPK) activity. In addition, these mutants have significantly lower IP kinase activity, indicating the successful conversion of IPK to GPK by structure-based engineering. Our work thus constitutes the first demonstration of a viable GPK enzyme with measurable FPK activity, which can be used in the chemoenzymatic synthesis of radiolabeled isoprenoid chains with potential application in research involving isoprenoid synthases and prenyltransferases.[7]

RESULTS AND DISCUSSION

Mutagenesis of THA IPK. Four mutants that contained different combinations of alanine substitutions for residues

Received: March 7, 2012
Accepted: April 25, 2012
Published: April 25, 2012

   dx.doi.org/10.1021/cb300106e | *ACS Chem. Biol.* 2012, 7, 1241−1246

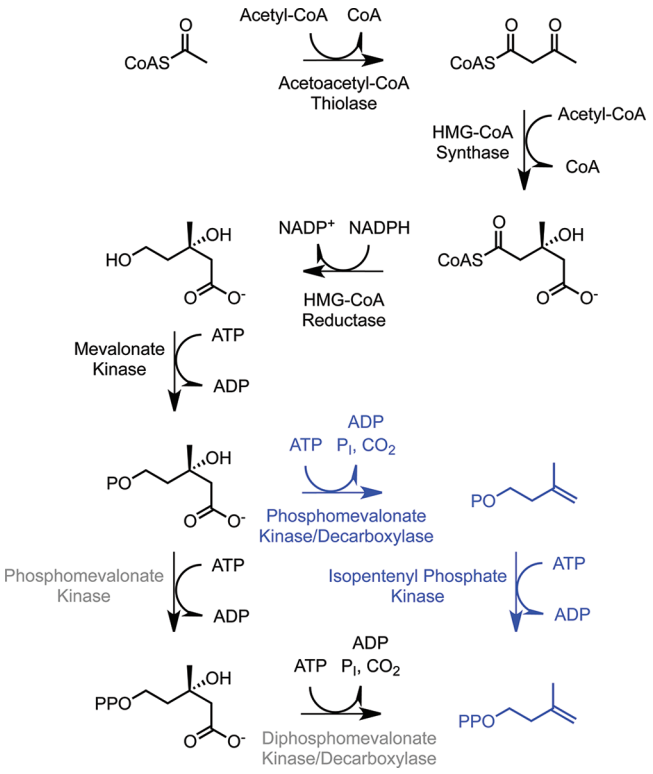

Figure 1. Archaeal mevalonate (MVA) pathway. Orthologs of the first four enzymes are found in the genomes of Archaea. The two enzymes (gray) required to convert mevalonate phosphate to IPP are generally missing in Archaea. An alternate route in the archaeal MVA pathway (blue) consisting of a putative phosphomevalonate decarboxylase and isopentenyl phosphate kinase has been proposed to complete the pathway.

Tyr70, Val73, Val130, and Ile140 were created. Tyr70 and Val73 are found on the long αC helix, and Val130 and Ile140 are on strands β9 and β10, respectively (Figure 2).[6] These

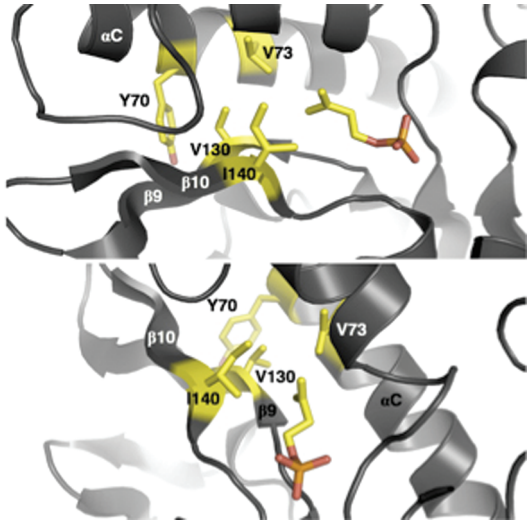

Figure 2. Alternate views of the isopentenyl phosphate (IP) binding site showing bulky amino acid residues (yellow sticks) mutated to alanine to accommodate the longer isoprenoid chains of geranyl phosphate (GP) and farnesyl phosphate (FP). Tyr70 and Val73 reside on helix αC, while Val130 and Ile140 are found on strands β9 and β10, respectively. The native substrate, IP, is shown as sticks.

residues are located at the distal end of the binding pocket for the isopentenyl moiety in IP. Val73, Val130, and Ile140 are near the bottom of the pocket, and on the basis of inspection of the structure, mutation of these residues appeared to be necessary to enlarge the pocket so that it would bind a geranyl unit. Inspection also suggested that the Y70A mutation is needed to accommodate a fully extended farnesyl unit. Table 1 lists the

Table 1. Mutants of *T. acidophilum* Isopentenyl Phosphate Kinase (THA IPK) and Combinations of Mutations in the IP Binding Site

mutant	combination of residues mutated to alanine
$YV_{130}I$	Tyr70, Val130, Ile140
$V_{73}V_{130}I$	Val73, Val130, Ile140
$YV_{73}V_{130}I$	Tyr70, Val73, Val130, Ile140
$YV_{73}I$	Tyr70, Val73, Ile140

mutations contained in each IPK variant. Mutants $YV_{73}V_{130}I$, $YV_{73}I$, and $YV_{130}I$ include the Y70A mutation. $V_{73}V_{130}I$ does not include the Y70A mutation and was expected to have minimal FP kinase activity. $YV_{73}V_{130}I$ also includes all of the different combinations of V73A, V130A, and I140A mutations found in the other three variants. Each mutant was purified to homogeneity (Figure 3a), and its ability to phosphorylate GP

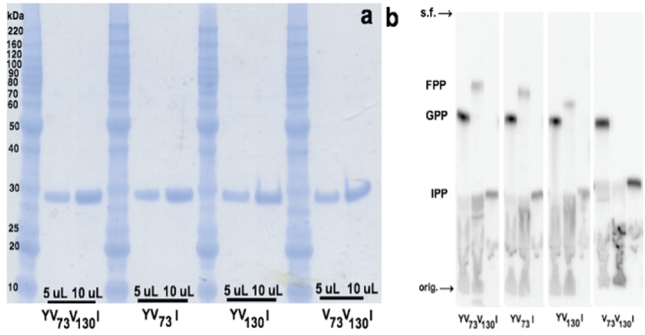

Figure 3. Purification of $YV_{73}V_{130}I$, $YV_{73}I$, $YV_{130}I$, and $V_{73}V_{130}I$ and autoradiography assays using [γ-^{32}P]ATP. (a) Denaturing sodium dodecyl sulfate–polyacrylamide gel electrophoresis of the four mutants. The masses of molecular mass markers are indicated. Monomeric THA IPK mutants have masses of ~29 kDa. (b) Autoradiogram showing production of GPP (lane 1), FPP (lane 2), and IPP (lane 3) by each of the mutants; orig. = origin, s.f. = solvent front.

and FP was determined by autoradiography using [γ-^{32}P]ATP (Figure 3b). All four mutants exhibited strong GP kinase activity, as shown by an intense spot corresponding to GPP (R_f = 0.52). In addition, $YV_{73}V_{130}I$, $YV_{73}I$, and $YV_{130}I$, each containing the Y70A mutation, showed detectable FP kinase activity (a less intense spot; R_f= 0.75), while $V_{73}V_{130}I$ without the Y70A mutation did not. Phosphorylation of GP appeared to be favored over that of FP or IP. These results indicate that the proteins fold into catalytically competent structures.

Kinetic Studies. GP and FP kinase activities of $YV_{73}V_{130}I$, $YV_{73}I$, $YV_{130}I$, and $V_{73}V_{130}I$ were measured using the coupled fluorescence assay of Pilloff et al.,[9,10] and the results are summarized in Table 2. Values of k_{cat} and K_M for GP, FP, and IP were measured at a saturating ATP concentration of 250 μM.

Mutant $YV_{73}V_{130}I$. $YV_{73}V_{130}I$ exhibited improved GP kinase activity compared to wild-type IPK. For this mutant, a k_{cat} of 1.1

Table 2. Kinetic Constants of *T. acidophilum* Isopentenyl Phosphate Kinase (THA IPK) Mutants for the Phosphorylation of Isopentenyl Phosphate (IP), Geranyl Phosphate (GP), and Farnesyl Phosphate (FP)[a]

		k_{cat} (s^{-1})	K_M (μM)	k_{cat}/K_M (M^{-1} s^{-1})
wild-type THA IPK				
	GP	0.05	$(4.7 \pm 1.3) \times 10^3$	10.0
	FP	not determined	not determined	not determined
	IP	8.0	4.4 ± 0.5	1.8×10^6
$YV_{73}V_{130}I$				
	GP	1.1 ± 0.1	$(2.4 \pm 0.3) \times 10^3$	4.7×10^2
	FP	0.6 ± 0.1	$(1.8 \pm 0.1) \times 10^3$	3.4×10^2
	IP	$(2.6 \pm 0.1) \times 10^{-3}$	$(5.3 \pm 0.8) \times 10^3$	0.5
$YV_{73}I$				
	GP	4.1 ± 0.2	$(3.5 \pm 0.3) \times 10^3$	1.2×10^3
	FP	1.4 ± 0.1	$(1.6 \pm 0.3) \times 10^3$	8.8×10^2
	IP	$(1.0 \pm 0.6) \times 10^{-2}$	$(7.9 \pm 0.1) \times 10^3$	1.3
$YV_{130}I$				
	GP	10.1 ± 0.7	$(8.0 \pm 1.1) \times 10^3$	1.3×10^3
	FP	1.4 ± 0.1	$(1.5 \pm 0.2) \times 10^3$	9.9×10^2
	IP	$(4.8 \pm 0.3) \times 10^{-3}$	$(5.7 \pm 0.9) \times 10^3$	0.9
$V_{73}V_{130}I$				
	GP	2.8 ± 0.5	$(9.5 \pm 2.7) \times 10^3$	3.0×10^2
	FP	not determined	not determined	not determined
	IP	$(1.1 \pm 0.1) \times 10^{-2}$	$(4.2 \pm 0.7) \times 10^3$	2.6

[a]Measurements were performed at a saturating ATP concentration of 250 μM.

$\pm$ 0.1 s^{-1} represents a 22-fold increase relative to the GP kinase activity for wild-type THA IPK.[10] In addition, K_M^{GP} = $(2.4 \pm 0.3) \times 10^3$ μM for $YV_{73}V_{130}I$, a slight change from the K_M^{GP} for the wild-type enzyme. The resulting catalytic efficiency is almost 50-fold larger than that for the wild-type enzyme. The k_{cat}^{FP} for phosphorylation by this mutant is 2 times lower than the k_{cat}^{GP} for the same enzyme. Because the GP kinase activity of wild-type THA IPK was very low, it was presumed that its promiscuous FP kinase activity would be negligible in comparison. The catalytic efficiency of $YV_{73}V_{130}I$ for the phosphorylation of FP is comparable to that for phosphorylation of GP. This mutant also exhibited a measurable yet weak residual IP kinase activity that is 3100-fold lower than that of wild-type THA IPK. Moreover, the K_M^{IP} of $YV_{73}V_{130}I$ is 1200-fold higher than that of wild-type THA IPK, resulting in a 10^6-fold decrease in k_{cat}^{IP}/K_M^{IP}. The k_{cat}^{ATP} and K_M^{ATP} for $YV_{73}V_{130}I$ using GP, FP, and IP as cosubstrates are similar to those for wild-type THA IPK (Supporting Information). The Michaelis–Menten curves for $YV_{73}V_{130}I$ (and other mutants) using GP, FP, or IP and ATP as cosubstrates are found in the Supporting Information.

Mutant $YV_{73}I$. $YV_{73}I$ exhibited improved GP kinase activity compared to $YV_{73}V_{130}I$, with a k_{cat}^{GP} of 4.1 ± 0.2 s^{-1} that is 90-fold greater than the k_{cat}^{GP} for wild-type THA IPK, and just half of the k_{cat}^{IP} for wild-type THA IPK. The Michaelis constant [K_M^{GP} = $(3.5 \pm 0.3) \times 10^3$ μM] is similar to those for $YV_{73}V_{130}I$ and wild-type THA IPK, resulting in a catalytic efficiency for GP kinase activity that is 3- and 120-fold greater than those of $YV_{73}V_{130}I$ and wild-type THA IPK, respectively. This GP kinase efficiency is only 10^3-fold lower than that of the native IP kinase activity of THA IPK and represents a significant activity for GP relative to the native enzyme. The FP kinase activity of $YV_{73}I$ is similar to that of $YV_{73}V_{130}I$, and its catalytic efficiency is only slightly lower than that of $YV_{73}V_{130}I$. The residual IP kinase activity of $YV_{73}I$ is slightly higher than that of $YV_{73}V_{130}I$, and its catalytic efficiency is 10^6-fold lower than that of wild-type THA IPK.

Similar to the profile observed for $YV_{73}V_{130}I$, the mutations in the IP binding site did not affect the kinetic parameters for ATP in the presence of the three different isoprenoid phosphate substrates. The k_{cat} and K_M values calculated for changes in ATP concentration for $YV_{73}I$ are similar to those measured for $YV_{73}V_{130}I$, the other two mutants ($YV_{130}I$ and $V_{73}V_{130}I$), and native THA IPK.

Mutant $YV_{130}I$. Among all four mutants tested, $YV_{130}I$ had the highest k_{cat}^{GP} (10.1 ± 0.7 s^{-1}), similar to the k_{cat}^{IP} for wild-type THA IPK and more than twice the activity of $YV_{73}I$ for GP. This is also more than 200-fold greater than the promiscuous activity of wild-type THA IPK for GP. K_M^{GP} = $(8.0 \pm 1.1) \times 10^3$ μM for $YV_{130}I$, leading to a catalytic efficiency that is only 10^3-fold lower than that of wild-type THA IPK for its native substrate, IP. The turnover number and Michaelis constant for FP with $YV_{130}I$ are similar to those for $YV_{73}I$. Finally, the remnant IP kinase activity is also similar to those of the previous mutants, with a low k_{cat}^{IP} that is almost 2000-fold lower than that for wild-type IPK. K_M^{IP} for $YV_{130}I$ is also 2000-fold higher than that for wild-type THA IPK but similar to those measured for $YV_{73}V_{130}I$ and $YV_{73}I$.

Mutant $V_{73}V_{130}I$. Among the four mutants, $V_{73}V_{130}I$ did not contain the Y70A mutation, resulting in a smaller substrate-binding site that was presumably unable to bind FP unless the hydrocarbon chain was in a more compact conformation. Modeling studies suggested that the active site of this mutant is sufficiently large to bind a fully extended GP. On the other hand, synthesis of FPP was not detected for $V_{73}V_{130}I$ in assays using [γ-^{32}P]ATP (Figure 3b). The k_{cat}^{GP} of 2.8 ± 0.5 s^{-1} for $V_{73}V_{130}I$ reflects a 60-fold improvement in turnover number relative to that of wild-type THA IPK. K_M^{GP} = $(9.5 \pm 0.3) \times 10^3$ μM, resulting in a 30-fold increase in catalytic efficiency for the phosphorylation of GP relative to the wild-type enzyme. The k_{cat} for $V_{73}V_{130}I$ for IP is almost 10^3-fold lower than that for wild-type THA IPK, and the K_M^{IP} is significantly higher than that for wild-type THA IPK. These result in a catalytic efficiency for the phosphorylation of IP by $V_{73}V_{130}I$ that is more than 70000-fold lower than that for wild-type THA IPK.

UPLC–MS Detection of GPP and FPP Products of IPK Mutants. The ability of each IPK mutant to produce the isoprenoid diphosphate products from their respective isoprenoid monophosphate substrates was confirmed by negative ion UPLC–MS using a C18 column. The chromatograms for synthesis of GPP gave peaks at 1.11 min for GPP (m/z 313, $C_{10}H_{19}P_2O_7^-$) and 3.39 min for GP (m/z 233, $C_{10}H_{18}PO_4^-$), while those for synthesis of FPP gave peaks at 4.74 min for FPP (m/z 381, $C_{15}H_{27}P_2O_7^-$) and 5.43 min for FP (m/z 301, $C_{15}H_{26}O_4P^-$). IPP and IP could not be separated on C_{18} or C_4 columns, but masses for the negative ion forms of IPP (m/z 245, $C_5H_{11}P_2O_7^-$) and IP (m/z 165, $C_5H_{10}PO_3^-$) were detected in the void volume (see the Supporting Information).

IPK Mutants with Triple Isoprenoid Monophosphate Kinase Activities. A total of four THA IPK mutants were created by structure-based redesign of the THA IPK active site by replacement of bulky amino acids in the IP binding site with alanine.[6] The IPK variants phosphorylate GP and FP,

dx.doi.org/10.1021/cb300106e | ACS Chem. Biol. 2012, 7, 1241–1246

isoprenoid chains that are longer than IP. These enzymes should be useful for the synthesis of β-^{32}P-labeled isoprenoid diphosphates and related molecules. The mutant kinases might also be useful in vivo for recycling isoprenoid monophosphates formed by hydrolysis of the corresponding diphosphates.[7,11,12]

Expansion of the IP binding site was based on the 2.0 Å crystal structure of THA IPK.[6] For all of the mutants, K_M^{IP} increased ~10^3-fold while k_{cat}^{IP} decreased by a similar magnitude. The increase in K_M^{IP} might have resulted from the increase in the size of the IP binding site that would allow IP to bind in a variety of unproductive conformations or have unfavorable interactions with water molecules in the enlarged active site. In contrast, modest changes in K_M^{GP} were observed in the THA IPK mutants relative to wild-type THA IPK, while the rate of turnover of GP increased 23−214-fold. Thus, the expansion of the hydrocarbon pocket in the active site allowed GP to bind in an orientation that facilitated phosphorylation.

Figure 4a shows a stable binding mode of GP in the $YV_{130}I$ active site determined by molecular dynamics calculations,

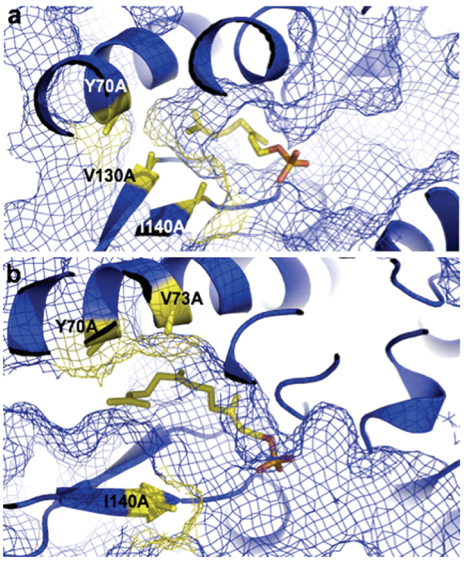

Figure 4. Binding conformations of geranyl phosphate (GP) and farnesyl phosphate (FP) in the active sites of two THA IPK mutants. (a) Mesh representation of the GP binding site of $YV_{130}I$. This mutant exhibited the highest k_{cat}^{GP} among the four THA IPK variants. (b) Mesh representation of the FP binding site of $YV_{73}I$. The FP molecule is not fully extended in this binding mode, although the Y70A mutation may allow its binding in this conformation.

where it appears that the alanine mutations created an expanded binding site sufficient to bind a kinked conformer of GP. Among the enzymes studied, $YV_{130}I$ exhibited the highest k_{cat}^{GP}, which is comparable to the k_{cat}^{IP} of wild-type THA IPK.[10] The other mutants had slightly lower GP kinase activities. Analysis of the products by UPLC−MS showed a >80% conversion to products at substrate concentrations of 2 mM GP and 5 mM ATP. It was observed that the three mutants with the highest GP kinase activities ($YV_{130}I$, $YV_{73}I$, and $V_{73}V_{130}I$) had smaller substrate binding pockets than $YV_{73}V_{130}I$ and suggested that a larger cavity did not necessarily translate to a higher activity. It was also observed that the mutants including the Y70A mutation had FP kinase activities that were weaker than their corresponding GP kinase activities. While our initial modeling experiments suggested that the Y70A mutation could permit FP to bind in an extended conformation, molecular dynamics simulations particularly of the binding of FP to the active site of $YV_{73}I$ showed that FP could also bind in a kinked conformation in the presence of the Y70A mutation, in a manner that does not fully exploit the available space resulting from the mutations.

Our steady-state measurements showed that $YV_{130}I$, $YV_{73}V_{130}I$, and $YV_{73}I$ have K_M^{FP} values that were lower than K_M^{GP}. FP binding might have been enhanced by van der Waals interactions between the long isoprenoid chain and the hydrophobic walls of the active site and turnover relative to GP limited by unfavorable conformations or slow product release. We also observed that the kinetic parameters for ATP of the mutants were similar to those of wild-type THA IPK, regardless of the cosubstrate. This is reasonable because the mutations were confined to the hydrocarbon pocket in the IP binding site, and there were no obvious interactions between ATP and the monophosphate substrates aside from their terminal phosphate groups.

Our results complement a previous report by Dellas and Noel in which novel FP kinase activities were achieved by mutagenesis of MJ IPK.[7] We have shown that analogous mutations in the THA IPK enzyme would result in GP kinase activities that are stronger than their coexistent FP kinase activities, producing both GPP and FPP. Other groups have reported the existence of isoprenol kinases that are able to catalyze the successive phosphorylation of farnesol and geranylgeraniol to the corresponding diphosphates using ATP, GTP, UTP, or CTP as a cosubstrate. These enzymes probably salvage isoprenoid alcohols for prenyl transfer reactions.[13−17]

CONCLUSION

Through the structure-based redesign of the IP binding site of THA IPK, we constructed four variants with improved catalytic activities for phosphorylation of GP and FP. In each case, the size of the hydrophobic pocket in the IP binding site was expanded by replacement of the wild-type amino acid with alanine. These changes resulted in a reduced catalytic efficiency for phosphorylation of IP through a decrease in k_{cat}^{IP} and an increase in K_M^{IP}. While similar decreases were seen for K_M^{GP} for the mutants, their k_{cat}^{GP} values were substantially higher than that of wild-type IPK. In particular, $YV_{130}I$, for which the improvement in k_{cat}^{GP} is >200-fold, is a good catalyst for synthesis of GPP from GP.

METHODS

Mutation of THA IPK. Computer modeling was performed using UCSF CHIMERA[18] to build GP and FP in the active site of THA IPK with *in silico* mutations. The complex models were then energy-minimized using AMBER 11[19] with force field ff03 for protein, and the general AMBER force field (GAFF) for GP and FP. Atomic charges for GP and FP were derived from the AM1-BCC charge scheme using Antechamber. Mutagenesis was conducted using the QuikChange Lightning Multi-Site Directed Mutagenesis Kit (Agilent Technologies) and mutagenic primers designed with the QuikChange Primer Design Tool. The plasmid template contained the THA IPK gene in the pET28b vector with an appended N-terminal sequence MGSSHHHHHHSSGLVPRGS upstream of the IPK sequence. Mutant constructs were confirmed by sequencing at the University of Utah DNA Sequencing Core Facility.

Detection of GP and FP Kinase Activity. Purified THA IPK mutants were tested for GP, FP, and IP kinase activity by incubating each enzyme (10 μM) with the respective monophosphate (5 mM) in

100 mM HEPES buffer (pH 7.5) containing 10 mM β-mercaptoethanol, 10 mM $MgCl_2$, 1 mg/mL BSA, and 1 μM [γ-^{32}P]ATP for 2 h at 37 °C in a total volume of 50 μL. The reactions were quenched with 100 μL of 500 mM EDTA. A 10−20 μL portion of each incubate was spotted on silica plates and developed with a $CHCl_3$/pyridine/formic acid/H_2O mixture (30:70:16:10, v/v/v/v). The TLC plate was imaged for 24 h using a storage phosphor autoradiography cassette and visualized using a Typhoon 8600 variable mode imager (GE Healthcare).

Kinetic Characterization of THA IPK Mutants. The protocol for fluorescent assays was based on the procedure of Pilloff et al.[9] with slight modifications. The activities of coupling enzymes were determined by measuring the change in the absorbance of NADH at 339 nm. Different concentrations of lactate dehydrogenase (LDH) were prepared in 100 mM HEPES buffer (pH 7.5) containing 10 mM $MgCl_2$, 10 mM β-mercaptoethanol, 1 mg/mL BSA, 120 μM pyruvate, and 150 μM NADH at 37 °C, and different concentrations of pyruvate kinase (PK) were prepared in 100 mM HEPES buffer (pH 7.5) containing 10 mM $MgCl_2$, 10 mM β-mercaptoethanol, 1 mg/mL BSA, 1 mM PEP, 4 mM ADP, 150 μM NADH, and LDH at 37 °C. The rates measured in absorbance units per second were converted to specific activity (units per milliliter) by using the NADH extinction coefficient ε of 6.22 mM^{-1} cm^{-1}. For kinetic measurements, each solution contained 2.5 units of PK and 3 units of LDH in assay buffer [100 mM HEPES (pH 7.5) containing 10 mM $MgCl_2$, 10 mM β-mercaptoethanol, 1 mg/mL BSA, and 250 μM ATP (saturating)] and an appropriate amount of GP, FP, or IP. Reactions were initiated by adding mutant enzyme to a final volume of 200 μL. The reaction was monitored at 37 °C for 600 s by observing the change in fluorescence (λ_{ex} = 340 nm; λ_{em} = 460 nm) (FluoroMax, Jobin Yvon Horiba). The initial rates were measured from the linear portion of the curve (<15% consumption of the concentration-limiting substrate). The kinetic constants were determined by fitting initial rates to eq 1 using nonlinear regression in GraFit5[20]

$$\nu/[E] = k_{cat}[S]/([S] + K_M) \quad (1)$$

where ν is the initial rate, [E] is the total concentration of enzyme in the mixture, [S] is the concentration of the isoprenoid substrate, and K_M is the Michaelis constant. The concentration of ATP was chosen after performing similar experiments using saturating concentrations of the isoprenoid substrates.

UPLC−MS of THA IPK Mutant Products, GPP, and FPP. Samples for UPLC−MS of GPP, FPP, and IPP produced by THA IPK mutants were obtained by incubating each mutant (10 μM) with 2 mM GP, FP, or IP (as a control) in 100 mM HEPES buffer (pH 7.5) containing 100 mM $MgCl_2$, 10 mM β-mercaptoethanol, 1 mg/mL BSA, and 5 mM ATP at 37 °C for 2 h. The mixtures were then centrifuged at 4 °C and 3000 rpm to remove the enzyme using a 10000 molecular weight cutoff Centricon (Millipore). The collected fractions were flash-frozen and lyophilized overnight and then dissolved in minimal volume of 25 mM NH_4HCO_3. Isoprenoid diphosphate products (GPP, FPP, and IPP) were separated from substrates (GP, FP, and IP) on a C18 column (for GPP and FPP) and a C4 column (for IPP) on a Waters ACQUITY UPLC H-Class system with a TQ (tandem quadrupole) detector. Isocratic elution with a 95:5 mixture of 25 mM NH_4HCO_3 and acetonitrile was used to separate GPP and GP, while isocratic elution with a 90:10 mixture of 25 mM NH_4HCO_3 and acetonitrile was used to separate FPP and FP, each at a flow rate of 0.6 mL/min. For IPP and IP, isocratic elution with a 100% solution of 25 mM NH_4HCO_3 was performed. Peaks with masses corresponding to each substrate and product were detected by negative-ion (ES-) MS.

■ ASSOCIATED CONTENT

Supporting Information

Materials and methods; ^{31}P and ^{1}H NMR spectra of IP, GP, and FP; representative UPLC−MS for IPP (produced by YV73I); Michaelis−Menten curves for GP, FP, and IP; kinetic parameters for the ATP utilization by mutant IPKs; modeled GP and FP in the mutant active sites; and references. This material is available free of charge via the Internet at http://pubs.acs.org.

■ AUTHOR INFORMATION

Corresponding Author

*E-mail: poulter@chemistry.utah.edu.

Present Address

§Department of Biochemistry, Duke University Medical Center, Box 3711, Nanaline H. Duke Building, Research Drive, Durham, NC 27710.

Notes

The authors declare no competing financial interest.

■ ACKNOWLEDGMENTS

We thank the Center for High-Performance Computing at the University of Utah for computer time.

■ REFERENCES

(1) Grochowski, L. L., Xu, H., and White, R. H. (2006) *Methanocaldoccus jannaschii* uses a modified mevalonate pathway for biosynthesis of isopentenyl diphosphate. *J. Bacteriol. 188*, 3192−3198.

(2) Liang, P., Ko, T., and Wang, A. H. (2002) Structure, mechanism and function of prenyltransferases. *Eur. J. Biochem. 269*, 3339−3354.

(3) Sacchetini, J. C., and Poulter, C. D. (1997) Creating isoprenoid diversity. *Science 277*, 1788−1789.

(4) Ogura, K., and Koyama, T. (1998) Enzymatic aspects of isoprenoid chain elongation. *Chem. Rev. 98*, 1263−1276.

(5) Song, L., and Poulter, C. D. (1994) Yeast farnesyl diphosphate synthase: Site-directed mutagenesis of residues in highly conserved prenyltransferase domains I and II. *Proc. Natl. Acad. Sci. U.S.A. 91*, 3044−3048.

(6) Mabanglo, M. F., Schubert, H. L., Chen, M., Hill, C. P., and Poulter, C. D. (2010) X-ray structures of isopentenyl phsophate kinase. *ACS Chem. Biol. 5* (5), 517−527.

(7) Dellas, N. P., and Noel, J. P. (2010) Mutation of archaeal isopentenyl phosphate kinase highlights mechanism and guides phosphorylation of additional isoprenoid monophosphates. *ACS Chem. Biol. 5* (6), 589−601.

(8) O'Maille, P E., Chappell, J., and Noel, J. P. (2004) A single-vial analytical and quantitative gas chromatography-mass spectrometry assay for terpene synthases. *Anal. Biochem. 335*, 210−217.

(9) Pilloff, D., Dabovic, K., Romanowski, M. J., Bonanno, J. B., Doherty, M., Burley, S. K., and Leyh, T. S. (2003) The kinetic mechanism of phosphomevalonate kinase. *J. Biol. Chem. 278*, 4510−4515.

(10) Chen, M., and Poulter, C. D. (2010) Characterization of thermophilic Archaeal isopentenyl phosphate kinase. *Biochemistry 49*, 207−217.

(11) Song, L. (2006) A soluble form of phosphatase in *Saccharomyces cerevisiae* capable of converting farnesyl diphosphate into *E,E*-farnesol. *Appl. Biochem. Biotechnol. 128*, 149−158.

(12) Coleman, J. E. (1992) Structure and mechanism of alkaline phosphatase. *Annu. Rev. Biophys. Biomol. Struct. 21*, 441−483.

(13) Inoue, H., Korenaga, T., Sagami, H., Koyama, T., and Ogura, K. (1994) Phosphorylation of farnesol by a cell-free system from *Botryococcus braunii*. *Biochem. Biophys. Res. Commun. 200*, 1036−1041.

(14) Ohnuma, S., Watanabe, M., and Nishino, T. (1996) Identification and characterization of geranylgeraniol kinase and geranylgeranyl phosphate kinase from the Archaebacterium *Sulfolobus acidocaldarius*. *J. Biochem. 119*, 541−547.

(15) Westfall, D., Aboushadi, N., Shackelford, J. E., and Krisans, S. K. (1997) Metabolism of farnesol: Phosphorylation of farnesol by rat liver microsomal and peroxisomal fractions. *Biochem. Biophys. Res. Commun. 230*, 562−568.

(16) Bentinger, M., Grünler, J., Peterson, E., Swiezewska, E., and Dallner, G. (1998) Phosphorylation of farnesol in rat liver microsomes: Properties of farnesol kinase and farnesyl phosphate kinase. *Arch. Biochem. Biophys. 353*, 191−198.
(17) Tachibana, A., Tanaka, T., Taniguchi, M., and Oi, S. (1996) Evidence for farnesol-mediated isoprenoid synthesis regulation in a halophilic archaeon, *Halopherax volcanii*. *FEBS Lett. 379*, 43−46.
(18) Petterson, E. F., Goddard, T. D., Huang, C. C., Couch, G. S., Greenblatt, D. M., Meng, E. C., and Ferrin, T. E. (2004) UCSF Chimera: A visualization system for exploratory research and analysis. *J. Comput. Chem. 13*, 1605−1612.
(19) Case, D. A., Darden, T. A., Cheatham, T. E., III, Simmerling, C. L., Wang, J., Duke, R. E., Luo, R., Walker, R. C., Zhang, W., Merz, K. M., Roberts, B., Wang, B., Hayik, S., Roitberg, A., Seabra, G., Kolossváry, I., Wong, K. F., Paesani, F., Vanicek, J., Liu, J., Wu, X., Brozell, S. R., Steinbrecher, T., Gohlke, H., Cai, Q., Ye, X., Wang, J., Hsieh, M.-J., Cui, G., Roe, D. R., Mathews, D. H., Seetin, M. G., Sagui, C., Babin, V., Luchko, T., Gusarov, S., Kovalenko, A., and Kollman, P. A. (2010) *AMBER 11*, University of California, San Francisco.
(20) Leatherbarrow, R. J. (2001) *GraFit*, version 5, Erithacus Software Ltd., Horley, U.K.